Proceedings of the ASME 2023 Conference on Smart Materials,
Adaptive Structures and Intelligent Systems
SMASIS2023
September 11-13, 2023, Austin, Texas

SMASIS2023-117601

MONITORING VOLUMETRIC DEFECTS IN 3D BIOPRINTING USING VIDEO-BASED VIBROMETRY

Rayanne Taylor¹ and Jinki Kim¹*

¹Georgia Southern University, Statesboro, GA

ABSTRACT

Additive manufacturing technologies have the potential to revolutionize the manufacturing industry by making it easier to fabricate complex structures, high value, and low volume parts in various contexts. Bio-additive manufacturing is particularly promising, as it has enabled the 3D printing of human organs. Researchers have made progress by developing novel materials and printing strategies for additively manufacturing complicated mission-critical geometries. On the other hand, assessing the structural integrity of these bio-printed structures has been challenging, as destructive contact-based approaches may interfere with the manufacturing process and affect the original dynamics and quality of the bio-prints, due to the relatively soft and lightweight nature of bio-prints. Furthermore, the repeatability of measurement is significantly dependent on the quality of how the sensor is attached to the part. Non-contact methods, such as laser and X-ray based techniques, can provide measurements without adding mass to the part. However, lasers may produce inaccuracies due to reflection and absorption in translucent materials, which are often found in bio-constructs. Although there have been significant advances in non-contact methods for reliably identifying damages in bio-printed structures, particularly embedded defects, implementing these approaches in a straightforward way has been challenging. To advance the state-of-the-art, this study proposes a novel method that can reliably assess the damage properties without contact by using video-based vibrometry. Vibration signals can provide a comprehensive response of the target structure, including material properties and geometry changes due to embedded defects in bioprinting. By analyzing the phase shift of the pixel intensity in the video, the vibration characteristics that indicate surface and/or embedded defects can be assessed for the entire structure captured in the camera angle, without the need for multiple sensors to be installed on the structure. This research focuses on analyzing the vibration characteristics of a cube that

was manufactured by an extrusion-based bio-printer with pneumatic dispensing using sodium alginate based bioink. A high-speed camera and phase-based motion estimation technique are used to obtain experimental data on the vibration characteristics of the cube. Volumetric defects introduced by extrusion pressure irregularity and scaffolds with voids and their severities are identified by monitoring the vibration characteristics. These findings suggest that the proposed method could be utilized to effectively verify the structural integrity of additively manufactured organs during fabrication, which could enhance process optimization and operation safety. Future works include incorporating finite element model to compare its response characteristics for healthy and damaged models with the experimentally obtained results and identifying the detection sensitivity and limit with respect to parameters such as damage type and location.

Keywords: additive manufacturing, 3D bioprinting, computer vision, phase-based motion estimation, structural health monitoring, nondestructive evaluation, damage detection.

1. INTRODUCTION

Although there is a great need for transplant organs to save people's lives, the availability of such organs is limited, resulting in an extensive waiting list for life-saving treatment. As per the Health Resources and Services Administration, over 104,000 individuals in the US are awaiting life-saving organ transplants, whereas only about 42,000 transplants were carried out in 2022 due to a severe scarcity of organs, and about 17 people in the United States die each day while waiting for an organ transplant [1]. Obtaining an organ involves either receiving one from a deceased person who voluntarily donated and passed away in a

^{*} Address all correspondence to this author. E-mail: jinkikim@georgiasouthern.edu

manner that left the organs viable for transplantation, or from a living donor, but this option is only available for two specific organs and requires compatibility with the recipient.

Bio-additive manufacturing has emerged as a promising breakthrough in the biomedical sector for creating human organs via 3D printing [2-6]. Bioprinting, a type of 3D printing that utilizes a gel-like bio-ink containing live cell cultures, is used to produce living tissue [3,7–9]. The ability to bioprint organs on demand could signify that the supply of organs meets the demand, eliminating waitlists and long waiting periods, thereby saving many lives. Additionally, the use of a patient's cells for printed organs may reduce the risk of rejection and mitigate several post-transplant complications [8,9]. Nevertheless, the adoption of bio-printed organs on a large scale is challenging due to the inadequate print quality, which falls significantly below the strict transplanting standards. This is partially due to the absence of appropriate process monitoring techniques to guarantee the quality of bio-prints. The primary criteria to ensure the viability of a printed organ are to keep the cells alive throughout and after the printing process and to ensure that the organ has the correct shape and structural integrity to withstand the human body. This study will concentrate on the structural integrity of the bioprints.

Although much research has been conducted to evaluate the structural integrity of bio-printed structures, most of these studies have used destructive methods that require contact-based techniques like piezoelectric transducers or strain gauges inspired by structural health monitoring devices used in mechanical and civil structures [10-13]. However, since bioprints are relatively soft and lightweight, using contact-type sensors may not be ideal for bio-printing as they can interfere with the original dynamics of the bio-prints and affect the manufacturing process and its quality. Moreover, the accuracy of measurement is dependent on how the sensor is attached to the part, and traditional methods are not suitable for measurement during the manufacturing process. Although noncontact methods such as laser and X-ray based techniques can provide measurements without mass loading [14–16], lasers may not be accurate due to reflection and absorption with translucent materials commonly used in bio-constructs [16]. Additionally, X-ray based methods have safety restrictions if they are to be used repeatedly over an extended period.

Although there have been significant advancements, it remains difficult to accurately identify damage features, particularly embedded defects, using non-contact methods that are easy to implement. Additionally, traditional methods are not well-suited for in-situ measurement during manufacturing processes. To overcome these challenges and improve the current state-of-the-art, this research proposes a new method that can reliably evaluate damage properties without the need for contact by utilizing video-based vibrometry. Vibration signals provide a comprehensive response of the target structure, encompassing both material properties and geometry changes that may occur due to factors such as defects in bioprinting. A

high-speed video camera captures movements that may be imperceptible to the naked eye. Since the phase shift of the pixel intensity is inherently related to any motion detected in the video [17], the vibration characteristics that indicate surface and/or embedded defect occurrence may be assessed remotely for the entire structure captured in the camera view from a distance even for translucent objects often found in bioprinting [18], without requiring multiple sensors to be installed on the structure.

2. MATERIALS AND METHODS

2.1 Hydrogel Sample Fabrication

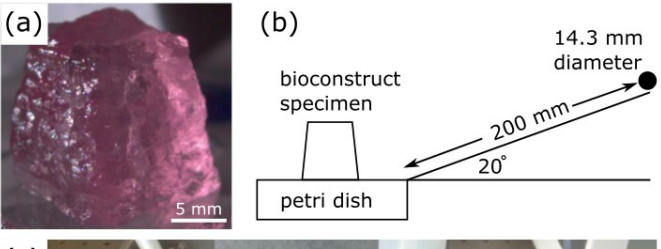
Sodium alginate (Alg) is a widely used material for cell viable bio-inks due to its biocompatibility and ability to modify rheological properties [19–21]. Sodium alginate is utilized either by itself [20] or in combination with other biocompatible materials such as gelatin [19]. In this study, sodium alginate (Sigma-Aldrich) solution in combination with carrageenan (Carr, Kitchen Alchemy), mainly composed of κ-Carr, is used as the bio-ink. Sodium alginate (3.5% w/v), carrageenan (2% w/v), and 1.109% w/v (0.1 M) calcium chloride (CaCl₂) solutions are respectively prepared in water. The sodium alginate and carrageenan solutions are first mixed until homogenous, then calcium chloride solution is mixed in about 20% at a time, until homogenous. The ratio of alginate to carrageenan to calcium chloride solutions at those concentrations is 10:10:1 by volume. The gel is created and stored at room temperature. The crosslinker (calcium chloride solution) was premixed to the bioink and it is not required to apply crosslinking solution after printed.

The study employed a pneumatic extrusion-based bioprinter (INKREDIBLE, Cellink) to create samples using the Alg-Carr-CaCl₂ composite bio-ink in an additive manner. This bio-ink is used without sterilization as a support material to test the feasibility of structures, which is similar to what is used in actual organ printing but lacks the ability to support live cells. The bio-ink was printed at room temperature with an extrusion pressure of 50 kPa through a dispensing needle nozzle with an inner diameter of 0.72 mm (19 gauge). All samples were printed on a glass petri dish.

The base shape of all the samples in this experiment is a 12.7 mm (0.5 in) cube with an eight-degree draft angle as illustrated in Fig. 1(a). Two types of volumetric damages were introduced by (1) printing a structure with a void near the center and (2) increasing the extrusion pressure at the point where the base sample print had progressed to 60%, emulating the print emulating nozzle clogs, which are one of the common defects occurred in bioprinting [22–24].

2.2 Experimental Set-up

Figure 1 illustrates the experimental set-up used in this study to confirm the efficacy of the proposed technique for monitoring volumetric damage in soft bioprinted samples. The vibration of the bioprinted samples is measured by a high-speed camera



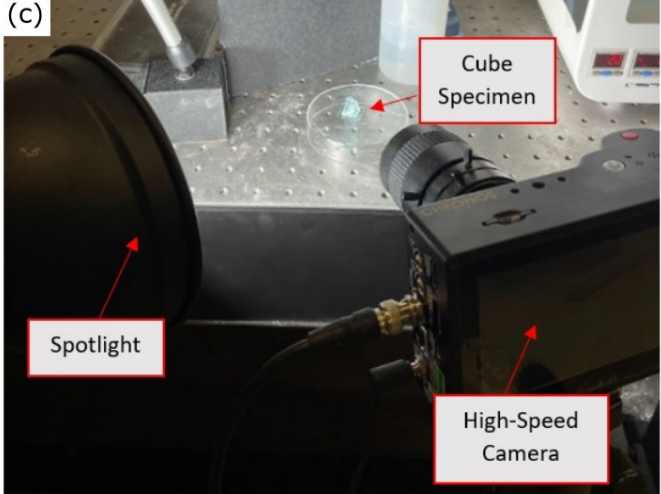


FIGURE 1: (A) HEALTHY BIOPRINT SAMPLE, (B) SKEMATIC OF THE SLIDE FOR BALL DROP EXCITATION, AND (C) EXPERIMENTAL SETUP.

(Chronos 1.4, Kron Technologies), which features a 1.3 megapixel CMOS sensor with a resolution of 1,280 × 1,024 pixels and a 12.5-75 mm f/1.2 zoom lens. The video's resolution $(416 \times 412 \text{ pixels})$ and frame rate (1,000 frames per second) were selected to capture as much spatiotemporal data as possible about the structure. The videos of the vibrating structures were recorded until the bioprinted sample settled, which typically took about 10 seconds after an impulsive excitation was applied. The impulse was applied by tapping the petri dish with a stainlesssteel ball (diameter, 14.3 mm) consistently dropped through a slide (200 mm length with 20° slope, shown in Fig. 1(b)). The camera was positioned roughly 300 mm away from the bioprinted sample to capture the entire motion of the vibrating structure within the camera's field of view, as depicted in Figure 1(c). Additionally, a DC-powered light fixture was used to provide extra illumination to the scene.

2.3 Phase Based Motion Estimation

The phase-based motion estimation technique [17,25,26] is used to analyze the movement of the bio-construct in the processed video. If lighting conditions remain consistent, the shift in pixel intensity in the frequency domain is directly linked to any motion that causes a variation in pixel intensity. The Fourier transform is employed as the basis function in this technique, which produces a global spatial transformation that can only handle global motions in the image sequence. However, complex steerable pyramid filters [27] can be used to identify the

localized amplitude and phase information of each pixel's intensities in the video's image sequences. This is achieved by using spatially localized Fourier transforms with different scales and orientations. By bandpassing each frame's pixel intensity I(x, y, t) using a complex filter $G_2^{\theta} + iH_2^{\theta}$, the local amplitude $A_{\theta}(x, y, t)$ and phase $\phi_{\theta}(x, y, t)$ at location (x, y) and time t can be determined.

$$(G_2^{\theta} + iH_2^{\theta}) \otimes I(x, y, t) = A_{\theta}(x, y, t)e^{i\phi_{\theta}(x, y, t)}$$
(1)

where G_2^{θ} and H_2^{θ} are the real and imaginary parts of the 2D complex filter for orientation θ .

This study employs 2D Gabor wavelet filters [25] as the basis function for localized Fourier transforms to obtain the local phase shifts of each pixel in the image sequence. This allows the identification of localized motions in both horizontal and vertical directions. The Gabor filters have two different orientations ($\theta = 0^{\circ}$ and 90°) and are decomposed in the video to generate the localized phase shifts. Figure 2 shows the Gabor filters used in the study.

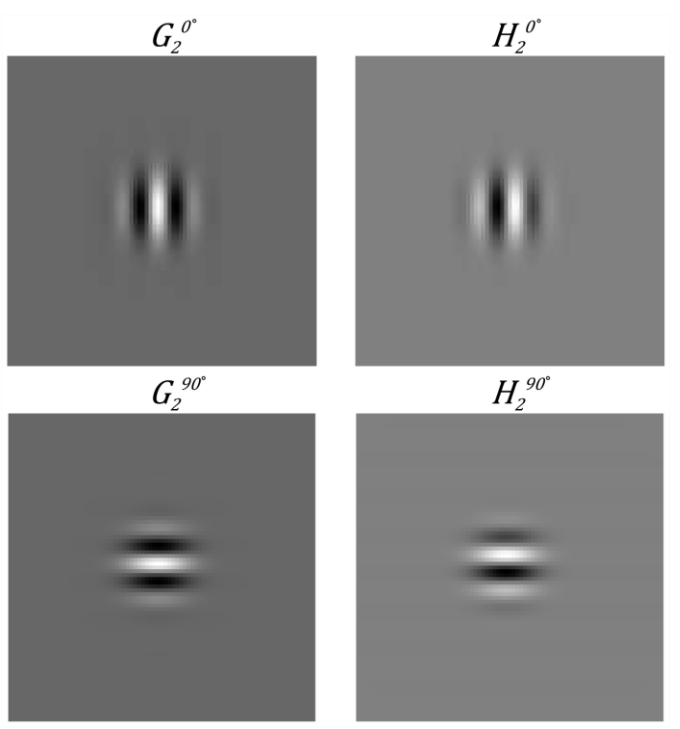


FIGURE 2. THE REAL AND IMAGINARY PAIRS OF 2D GABOR FILTERS FOR TWO DIFFERENT ORIENTATIONS (0° AND 90°), WHICH FILTERS THE HORIZONTAL AND VERTICAL MOTIONS, RESPECTIVELY. THE GRAY LEVEL CORRESPONDS TO THE VALUE OF THE FILTER.

To filter the displacement signals or local phase over time for each pixel in the video frames, a Tukey window is used with a cosine/constant section ratio of 0.1 for leakage protection and fair amplitude accuracy. This ratio is kept constant for all samples in the study. A fast Fourier transform is used to obtain

the individual spectral responses of the filtered signals for each pixel. These responses are then averaged in the frequency domain to obtain a single spectrum that represents the overall response of the bio-construct sample. To estimate the motion of the target structure, only regions with sufficient texture are used. assuming constant and even lighting conditions, as the intensity changes in each pixel of the image sequence are utilized for motion estimation. The mask is set by evaluating the gradient magnitude of the frame and pixels without texture are masked out from averaging to reduce the noise floor in the spectral domain. After obtaining the resonance frequency peaks from the spectral response, phase-based motion magnification [17] is used to estimate the mode shapes of the corresponding resonance frequencies. To decompose the local phase signals from the original video, a set of complex steerable pyramid filters [27] applied to the image sequence.

The local phase signals are subjected to temporal bandpass filtering within a frequency range that includes the resonance frequency. These signals are then multiplied by an amplification factor to magnify the motion of interest while minimizing noise. The amplification factor is manually selected to identify the mode shape while keeping noise to a minimum. The amplified phase signal is then combined with the amplitude signal to reconstruct a video, which results in an amplified visualization of the specific motion of interest. The motion-magnified video shows the operational deflection shape, which represents the corresponding mode shape [25] in a qualitative manner. The frequency band is selected carefully to include only the resonance frequency of interest. A detailed explanation of this method is available in the literature [17].

3. RESULTS AND DISCUSSION

3.1 Reliability of the Experimental Measurement

To evaluate the consistency of the experimental setup, the resonance frequencies of five bioprinted hydrogel samples without any defects were measured from each video.

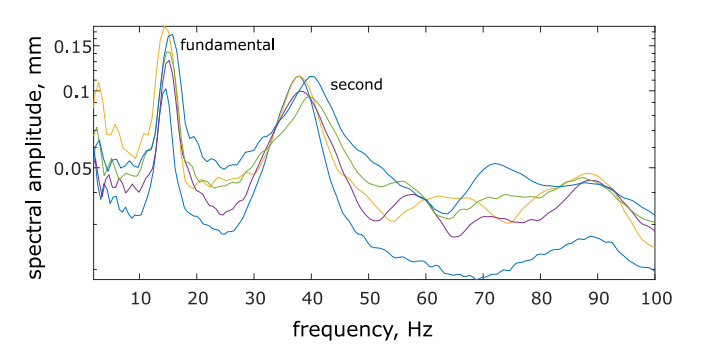


FIGURE 3. EXPERIMENTALLY OBTAINED FREQENCY RESPONSES OF FIVE HYDROGEL BIOCONSTRUCTS USING VIDEO-BASED VIBROMETRY.

Figure 3 provides an example of the frequency responses obtained by video-based vibrometry. The fundamental and second resonance frequencies respectively correspond to a transverse and longitudinal mode shapes of the bioconstructs. The resulting resonance frequencies obtained from each of the five samples are recorded in Table 1. The average resonance frequencies are determined to be 13.4 Hz and 39.1 Hz with standard deviations of 10% and 4%, respectively. These findings indicate that the experimental setup provides dependable fabrication and measurement of the hydrogel samples. Overall, the results demonstrate that the video-based approach is capable of delivering reliable measurements of the vibration characteristics of translucent bio-printed structures.

TABLE 1: FUNDAMENTAL AND SECOND RESONANCE FREQUENCIES OF FIVE HEALTHY SAMPLES USING VIDEO-BASED VIBROMETRY

Sample no.	1	2	3	4	5
Fundamental resonance, Hz	14.6	14.1	11.7	12.3	14.5
Second resonance, Hz	37.0	40.4	37.6	39.9	40.5

3.2 Experimental Investigations on the Damage Effect

The first type of volumetric defect evaluated in this study is cubic voids in the bioconstructs. These types of defects may be occurring due to irregularities in the bio-ink, extruding conditions, collapse of infill patterns, or delamination of the bio-ink. Cubic cavities are introduced near the center of the cubic samples as shown in Fig. 4(a), which cannot be readily detected by visually inspecting the surface of the scaffold sample. Figure 4(c) shows the experimentally measured fundamental and second resonance frequencies as a function of the damage size (length of the voids). It can be observed that the resonance frequencies decrease when greater void defect is introduced.

This follows the expected trend based on the well-known relationship for natural frequency $\omega_n = \sqrt{k_e/m_e}$, where k_e and m_e are the effective stiffness and mass of the target structure, respectively. While the void introduced in the bioconstructs will cause a slight decrease in the total mass of the specimen, the decrease in the resonance frequencies may be mainly attributed to the effective stiffness decrease, which is determined by the structural integrity.

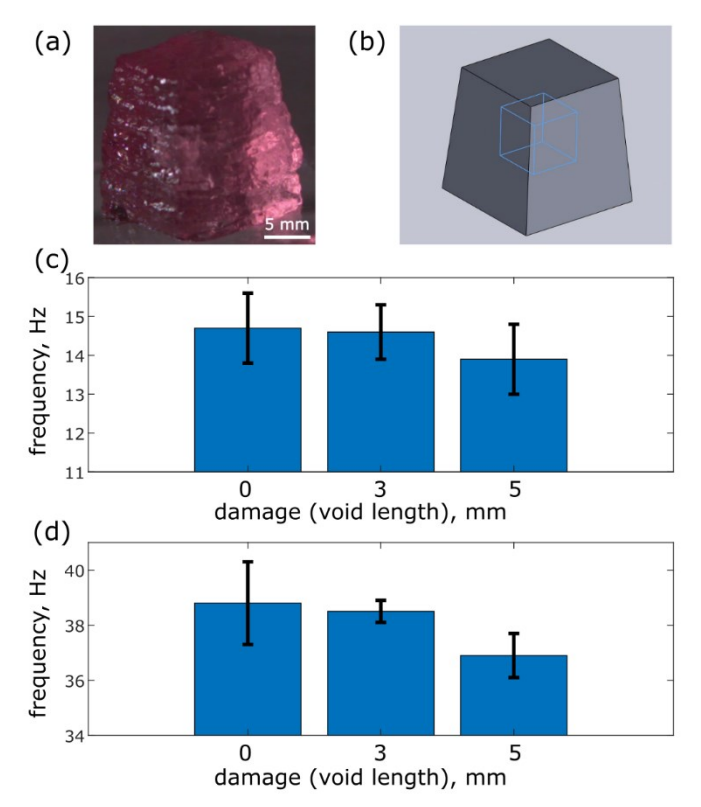


FIGURE 4. (A) BIOCONSTRUCT WITH VOID DEFECTS NEAR THE CENTER AND (B) ITS SLICED VIEW FROM THE CAD MODEL. EXPERIMENTALLY OBTAINED (C) FUNDAMENTAL AND (D) SECOND RESONANCE FREQUENCIES FOR HEALTHY AND DAMAGED BIOCONSTRUCTS WITH VOIDS. ERROR BARS INDICATE ONE STANDARD DEVIATION FROM THE MEAN VALUES OF THREE SAMPLES MEASURED FOR EACH CONDITION.

In addition, another defect type that may be introduced by irregularities in the extruding condition, such as clogging, pressure change, is investigated. In order to emulate such condition, the extrusion pressure was increased by 8 kPa respectively when the healthy samples are printed up to 60% of their total progress. The extrusion irregularity in the 3d printed construct cannot be readily identified by visually inspecting the surface. However, fundamental and second resonance frequencies decrease when greater extrusion pressure is applied in the printing process, as shown in Fig. 5. While the effective stiffness of the bio-construct, which is mainly determined by the structural integrity near the base, may not exhibit significant changes, the increased extrusion pressure resulting into increased mass near the top side of the bioconstructs will contribute to decreasing the resonance frequencies.

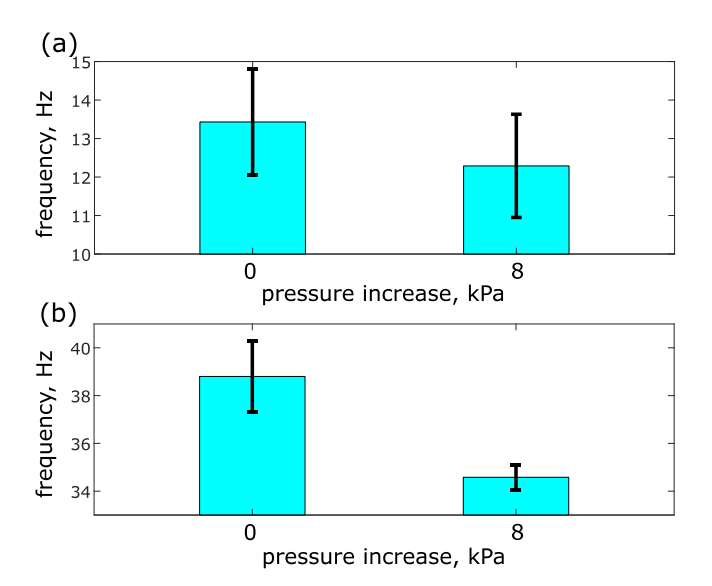


FIGURE 5. **EXPERIMENTALLY OBTAINED** (A) **FUNDAMENTAL** AND **SECOND** RESONANCE (B) **FREOUENCIES FOR** HEALTHY DAMAGED AND BIOCONSTRUCTS WITH PRESSURE IRREGULARITIES. ERROR BARS INDICATE ONE STANDARD DEVIATION FROM THE MEAN VALUES OF THREE SAMPLES MEASURED FOR EACH CONDITION.

Overall, the experimental outcomes support the efficacy of the proposed approach to determine the vibration features of bioprinted structures using video-based vibrometry. This technique is useful for detecting volumetric defects and assessing the structural integrity of bioconstructs in a noncontact and non-invasive way. Future works include (1) incorporating finite element model to compare its response characteristics for healthy and damaged models with the experimentally obtained results, (2) identifying the detection sensitivity and limit with respect to parameters such as bioconstruct shape, defect type and location, and (3) application to on-line defect detection. In addition, the mechanical properties of a 3D printed construct can be influenced by various complex factors, such as specific cell types, cell density and activity, the choice of biomaterials, and fabrication techniques used in bio 3D printing. For example, the proliferation of cells are affected by the mechanical stiffness of the biomaterial [28], and it is shown that the density of cells has an impact on mechanical stiffness [29]. The research group also plans to conduct studies to assess cell density and activity by measuring the vibration characteristics of the bioconstructs.

4. CONCLUSION

This study explores a novel technique for assessing the structural integrity of soft and translucent bio-constructs by analyzing their vibration characteristics using non-contact video-based vibrometry. The vibration characteristics of a cube made by an extrusion-based bio-printer with sodium alginate and

carrageenan-based bio-ink are measured using a high-speed camera and a phase-based motion estimation technique. The effectiveness of the experimental setup is confirmed by measuring multiple baseline samples without defects. Volumetric defects induced by voids and extrusion pressure irregularities are introduced and changes in the vibration characteristics are monitored to identify the presence and severity of defects. This research lays the groundwork for using video-based vibrometry for quality assurance in bioprinting organs, which could improve the accuracy of assessing the structural integrity of prints and lead to the creation of highquality bio-additive manufacturing. Future work will involve implementing the approach to verify the structural integrity of additively manufactured organs for various types of defects during fabrication. This could help optimize the process and operation safety, and ultimately advance public health and medical/pharmaceutical fields.

ACKNOWLEDGEMENTS

This research is supported by faculty research seed grant from the College of Engineering and Computing at Georgia Southern University.

REFERENCES

- [1] Health Resources & Service Administration, "Organ Donation Statistics" [Online]. Available: https://www.organdonor.gov/learn/organ-donation-statistics. [Accessed: 09-Apr-2023].
- [2] Hinton, T. J., Jallerat, Q., Palchesko, R. N., Park, J. H., Grodzicki, M. S., Shue, H. J., Ramadan, M. H., Hudson, A. R., and Feinberg, A. W., 2015, "Three-Dimensional Printing of Complex Biological Structures by Freeform Reversible Embedding of Suspended Hydrogels," Sci. Adv., 1(9).
- [3] Mirdamadi, E., Tashman, J. W., Shiwarski, D. J., Palchesko, R. N., and Feinberg, A. W., 2020, "FRESH 3D Bioprinting a Full-Size Model of the Human Heart," ACS Biomater. Sci. Eng., 6(11), pp. 6453–6459.
- [4] Ross, M. T., Cruz, R., Brooks-Richards, T. L., Hafner, L. M., Powell, S. K., and Woodruff, M. A., 2018, "Comparison of Three-Dimensional Scanning Techniques for Capturing the External Ear," Virtual Phys. Prototyp., 13(4), pp. 255–265.
- [5] Ahmad, M., Suardi, N., Shukri, A., Mohammad, H., Oglat, A., Alarab, A., and Makhamrah, O., 2020, "Chemical Characteristics, Motivation and Strategies in Choice of Materials Used as Liver Phantom: A Literature Review," J. Med. Ultrasound, 28(1), pp. 7–16.
- [6] Tuncay, V., and van Ooijen, P. M. A., 2019, "3D Printing for Heart Valve Disease: A Systematic Review," Eur. Radiol. Exp., 3(1), p. 9.
- [7] Heinrich, M. A., 2019, "3D Bioprinting: From Benches to Translational Applications," Small, **15**(23), p.

- 1805510.
- [8] Elalouf, A., 2021, "Immune Response against the Biomaterials Used in 3D Bioprinting of Organs," Transpl. Immunol., **69**(August), p. 101446.
- [9] Leberfinger, A. N., Dinda, S., Wu, Y., Koduru, S. V., Ozbolat, V., Ravnic, D. J., and Ozbolat, I. T., 2019, "Bioprinting Functional Tissues," Acta Biomater., 95, pp. 32–49.
- [10] Markidou, A., Shih, W. Y., and Shih, W. H., 2005, "Soft-Materials Elastic and Shear Moduli Measurement Using Piezoelectric Cantilevers," Rev. Sci. Instrum., 76(6).
- [11] Lee, D., Zhang, H., and Ryu, S., 2019, "Elastic Modulus Measurement of Hydrogels," *Cellulose-Based Superabsorbent Hydrogels*, pp. 865–884.
- [12] Kim, J., and Wang, K. W., 2014, "An Enhanced Impedance-Based Damage Identification Method Using Adaptive Piezoelectric Circuitry," Smart Mater. Struct., 23(9), p. 095041.
- [13] Kim, J., and Wang, K. W., 2019, "Electromechanical Impedance-Based Damage Identification Enhancement Using Integrated Bistable and Adaptive Piezoelectric Circuitry," Struct. Heal. Monit., 18(4), pp. 1268–1281.
- [14] Schwarz, S., and Hartmann, B., 2020, "Contactless Vibrational Analysis of Transparent Hydrogel Structures Using Laser-Doppler Vibrometry," Exp. Mech., 60, pp. 1067–1078.
- [15] Mansur, H. S., Oréfice, R. L., and Mansur, A. A. P., 2004, "Characterization of Poly(Vinyl Alcohol)/Poly(Ethylene Glycol) Hydrogels and PVA-Derived Hybrids by Small-Angle X-Ray Scattering and FTIR Spectroscopy," Polymer (Guildf)., **45**(21), pp. 7193–7202.
- [16] Ohtani, K., Li, L., and Baba, M., 2013, "Determining Surface Shape of Translucent Objects by Using Laser Rangefinder," 2013 IEEE/SICE Int. Symp. Syst. Integr. SII 2013, pp. 454–459.
- [17] Wadhwa, N., Rubinstein, M., Durand, F., and Freeman, W. T., 2013, "Phase-Based Video Motion Processing," ACM Trans. Graph., **32**(4).
- [18] Kim, J., Sapp, L., and Sands, M., 2022, "Simultaneous and Contactless Characterization of the Young's and Shear Moduli of Gelatin-Based Hydrogels," Exp. Mech., 62, pp. 1615–1624.
- [19] Kim, M. H., Lee, Y. W., Jung, W. K., Oh, J., and Nam, S. Y., 2019, "Enhanced Rheological Behaviors of Alginate Hydrogels with Carrageenan for Extrusion-Based Bioprinting," J. Mech. Behav. Biomed. Mater., 98(June), pp. 187–194.
- [20] Webb, B., and Doyle, B. J., 2017, "Parameter Optimization for 3D Bioprinting of Hydrogels," Bioprinting, 8(September), pp. 8–12.
- [21] Schwab, A., Levato, R., D'Este, M., Piluso, S., Eglin, D., and Malda, J., 2020, "Printability and Shape Fidelity of Bioinks in 3D Bioprinting," Chem. Rev., **120**(19), pp. 11028–11055.
- [22] Gillispie, G., Prim, P., Copus, J., Fisher, J., Mikos, A.

- G., Yoo, J. J., Atala, A., and Lee, S. J., 2020, "Assessment Methodologies for Extrusion-Based Bioink Printability," Biofabrication, **12**(2).
- [23] Fisch, P., Holub, M., and Zenobi-Wong, M., 2021, "Improved Accuracy and Precision of Bioprinting through Progressive Cavity Pump-Controlled Extrusion," Biofabrication, 13(1).
- [24] Afghah, F., Altunbek, M., Dikyol, C., and Koc, B., 2020, "Preparation and Characterization of Nanoclay-Hydrogel Composite Support-Bath for Bioprinting of Complex Structures," Sci. Rep., **10**(1), pp. 1–13.
- [25] Chen, J. G., Wadhwa, N., Cha, Y. J., Durand, F., Freeman, W. T., and Buyukozturk, O., 2015, "Modal Identification of Simple Structures with High-Speed Video Using Motion Magnification," J. Sound Vib., 345, pp. 58–71.
- [26] Poozesh, P., Sarrafi, A., Mao, Z., Avitabile, P., and Niezrecki, C., 2017, "Feasibility of Extracting Operating Shapes Using Phase-Based Motion Magnification Technique and Stereo-Photogrammetry," J. Sound Vib., 407, pp. 350–366.
- [27] Simoncelli, E. P., and Freeman, W. T., 1995, "Steerable Pyramid: A Flexible Architecture for Multi-Scale Derivative Computation," IEEE Int. Conf. Image Process., 3, pp. 444–447.
- [28] Zhang, J., Wehrle, E., Adamek, P., Paul, G. R., Qin, X. H., Rubert, M., and Müller, R., 2020, "Optimization of Mechanical Stiffness and Cell Density of 3D Bioprinted Cell-Laden Scaffolds Improves Extracellular Matrix Mineralization and Cellular Organization for Bone Tissue Engineering," Acta Biomater., 114, pp. 307–322.
- [29] You, S., Xiang, Y., Hwang, H. H., Berry, D. B., Kiratitanaporn, W., Guan, J., Yao, E., Tang, M., Zhong, Z., Ma, X., Wangpraseurt, D., Sun, Y., Lu, T. Y., and Chen, S., 2023, "High Cell Density and High-Resolution 3D Bioprinting for Fabricating Vascularized Tissues," Sci. Adv., 9(8), pp. 1–14.